

UvA-DARE (Digital Academic Repository)

A Novel, Nondestructive, Dried Blood Spot-Based Hematocrit Prediction Method Using Noncontact Diffuse Reflectance Spectroscopy

Capiou, S.; Wilk, L.S.; Aalders, M.C.G.; Stove, C.P.

DOI

[10.1021/acs.analchem.6b01321](https://doi.org/10.1021/acs.analchem.6b01321)

Publication date

2016

Document Version

Other version

Published in

Analytical Chemistry

[Link to publication](#)

Citation for published version (APA):

Capiou, S., Wilk, L. S., Aalders, M. C. G., & Stove, C. P. (2016). A Novel, Nondestructive, Dried Blood Spot-Based Hematocrit Prediction Method Using Noncontact Diffuse Reflectance Spectroscopy. *Analytical Chemistry*, *88*(12), 6538-6546.
<https://doi.org/10.1021/acs.analchem.6b01321>

General rights

It is not permitted to download or to forward/distribute the text or part of it without the consent of the author(s) and/or copyright holder(s), other than for strictly personal, individual use, unless the work is under an open content license (like Creative Commons).

Disclaimer/Complaints regulations

If you believe that digital publication of certain material infringes any of your rights or (privacy) interests, please let the Library know, stating your reasons. In case of a legitimate complaint, the Library will make the material inaccessible and/or remove it from the website. Please Ask the Library: <https://uba.uva.nl/en/contact>, or a letter to: Library of the University of Amsterdam, Secretariat, P.O. Box 19185, 1000 GD Amsterdam, The Netherlands. You will be contacted as soon as possible.

UvA-DARE is a service provided by the library of the University of Amsterdam (<https://dare.uva.nl>)

Supporting Information Capiou *et al.*

**A novel, non-destructive, dried blood spot-based hematocrit prediction method
using non-contact diffuse reflectance spectroscopy**

Sara Capiou^{1*}, Leah S. Wilk^{2*}, Maurice C.G. Aalders², Christophe P. Stove¹.

**Equally contributed*

¹Laboratory of Toxicology, Faculty of Pharmaceutical Sciences, Ghent University, Ottergemsesteenweg 460,
9000 Ghent, Belgium.

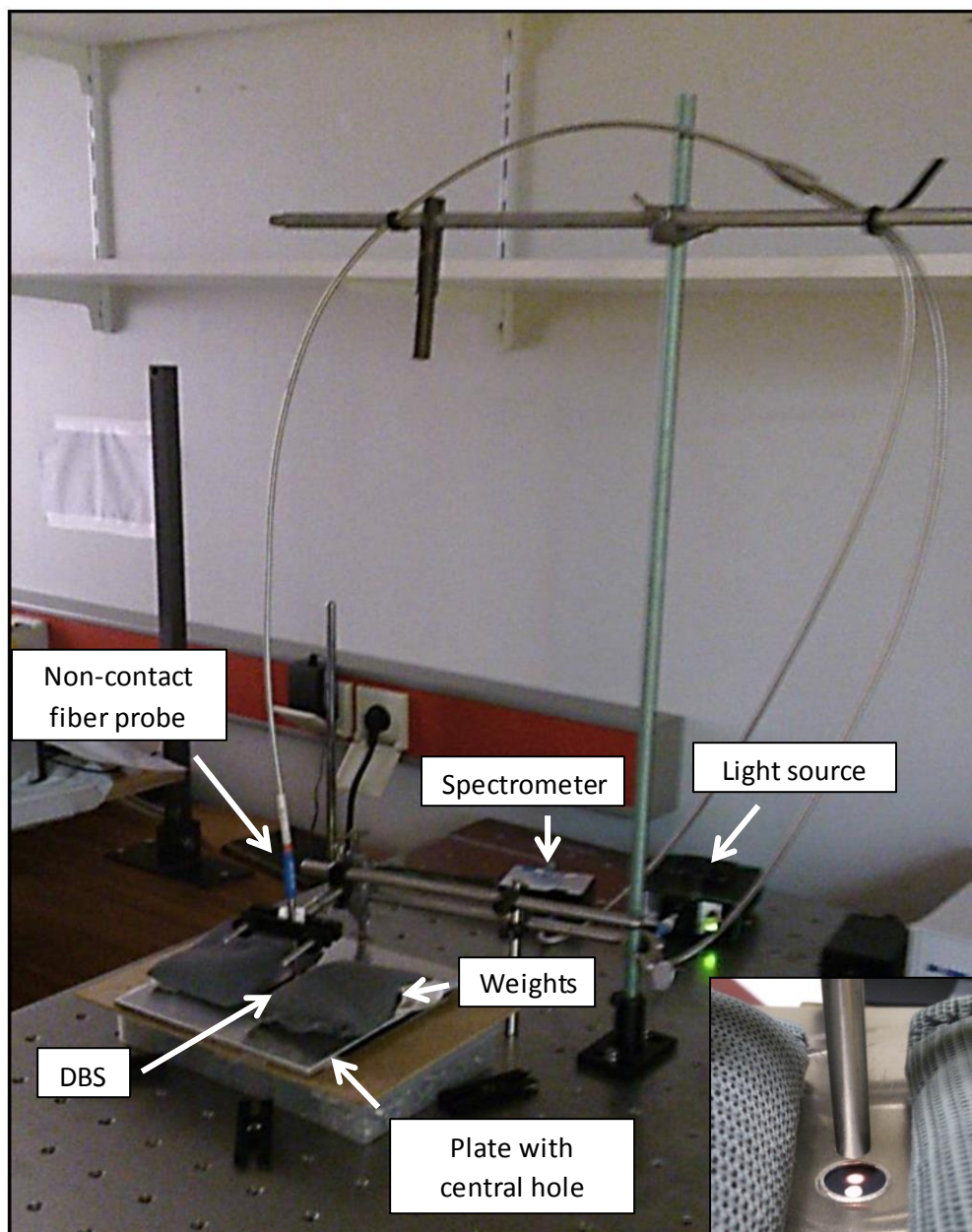
²Department of Biomedical Engineering and Physics, Academic Medical Center, University of Amsterdam,
Meibergdreef 9, 1105 AZ Amsterdam, The Netherlands.

CONTENT

Page S-2	Supplementary Figure S-1
Page S-3	Supplementary Figure S-2
Page S-4	Supplementary Table S-1
Page S-5	Supplementary Tables S-2A and S-2B
Page S-6	Supplementary Figure S-3
Page S-7	Supplementary Figure S-4A
Page S-8	Supplementary Figure S-4B
Page S-9	Supplementary Table S-3
Page S-10	Supplementary Figure S-5
Page S-11	Supplementary Figure S-6
Page S-12	Supplementary Figure S-7

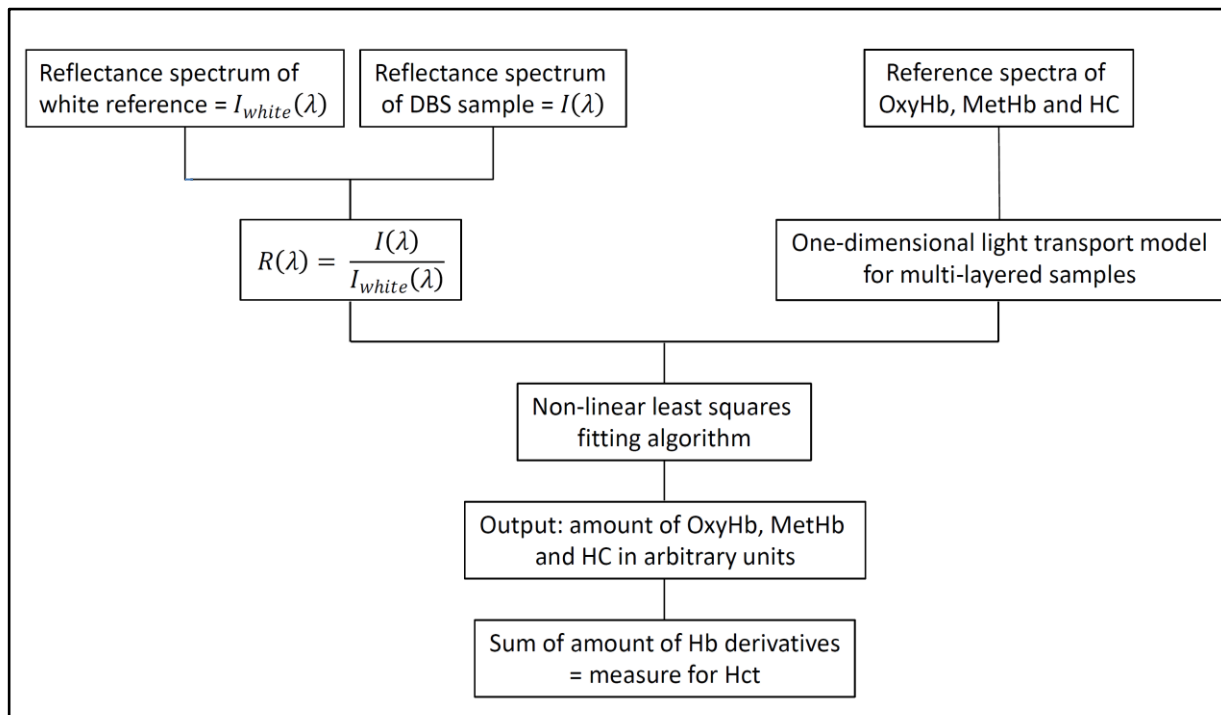
Supplementary Figure S-1

Depicted is a photograph of the utilized set-up on which the different parts required for the analysis are indicated. The inserted photograph in the right bottom corner is a close-up of the optical probe when the measuring distance was set at 0.7 cm and the illuminated area was 3-mm. Below the 3-mm illuminated spot, a 3-mm DBS punch was positioned as a size-reference. Also visible is the black background on which the DBS samples are positioned during analysis.



Supplementary Figure S-2

Depicted is a flow chart of how the spectral data analysis is performed.



Supplementary Table S-1**Table S-1: Overview of the Hct values (measured with a Sysmex XE-5000 hematology analyzer) of all calibrators and QCs (in Li-heparin-anticoagulated blood) prepared for the evaluation of accuracy and precision.**

	Day 1	Day 2	Day 3
Donor 1			
Calibration curve 1	0.20, 0.27, 0.35, 0.42, 0.50, 0.57, 0.66	0.21, 0.28, 0.36, 0.43, 0.52, 0.59, 0.67	0.20, 0.28, 0.35, 0.41, 0.52, 0.59, 0.68
QCs 1	0.20, 0.43, 0.66	0.21, 0.43, 0.67	0.20, 0.43, 0.69
Calibration curve 2	0.20, 0.27, 0.35, 0.42, 0.50, 0.57, 0.65	0.21, 0.28, 0.36, 0.43, 0.52, 0.59, 0.68	0.20, 0.28, 0.36, 0.43, 0.52, 0.59, 0.69
QCs 2	0.20, 0.42, 0.65	0.20, 0.44, 0.68	0.20, 0.43, 0.67
Donor 2			
Calibration curve 1	0.20, 0.27, 0.35, 0.42, 0.50, 0.57, 0.65	0.20, 0.27, 0.34, 0.42, 0.50, 0.58, 0.66	0.19, 0.26, 0.34, 0.41, 0.48, 0.54, 0.63
QCs 1	0.20, 0.42, 0.65	0.20, 0.42, 0.66	0.19, 0.40, 0.64
Calibration curve 2	0.20, 0.27, 0.35, 0.42, 0.50, 0.57, 0.65	0.20, 0.27, 0.35, 0.42, 0.50, 0.57, 0.65	0.19, 0.26, 0.33, 0.40, 0.49, 0.56, 0.65
QCs 2	0.20, 0.41, 0.65	0.20, 0.42, 0.65	0.20, 0.40, 0.64
Donor 3			
QCs 1	0.20, 0.44, 0.68	0.20, 0.42, 0.66	0.20, 0.42, 0.66
QCs 2	0.21, 0.44, 0.70	0.20, 0.42, 0.65	0.20, 0.42, 0.67
Donor 4			
QCs 1	0.18, 0.39, 0.61	0.20, 0.42, 0.66	0.19, 0.40, 0.65
QCs 2	0.18, 0.39, 0.62	0.20, 0.43, 0.66	0.19, 0.41, 0.66
Donor 5			
QCs 1	0.19, 0.41, 0.63	0.19, 0.41, 0.64	0.19, 0.42, 0.64
QCs 2	0.19, 0.40, 0.63	0.19, 0.41, 0.64	0.20, 0.42, 0.65
Donor 6			
QCs 1	0.19, 0.40, 0.62	0.19, 0.40, 0.62	0.20, 0.42, 0.68
QCs 2	0.19, 0.40, 0.63	0.18, 0.39, 0.60	0.20, 0.43, 0.67

Supplementary Tables S-2A en S-2B

The equation used to calculate the normalized predicted Hct is depicted below (Eq. S-1). An example of its implementation can be found in tables S-2A and S-2B.

$$\text{Normalized predicted Hct} = \frac{\text{Predicted Hct} \times \text{Average true Hct}}{\text{True Hct}} \quad (\text{Eq. S-1})$$

Table S-2A: Original true and predicted Hct values.

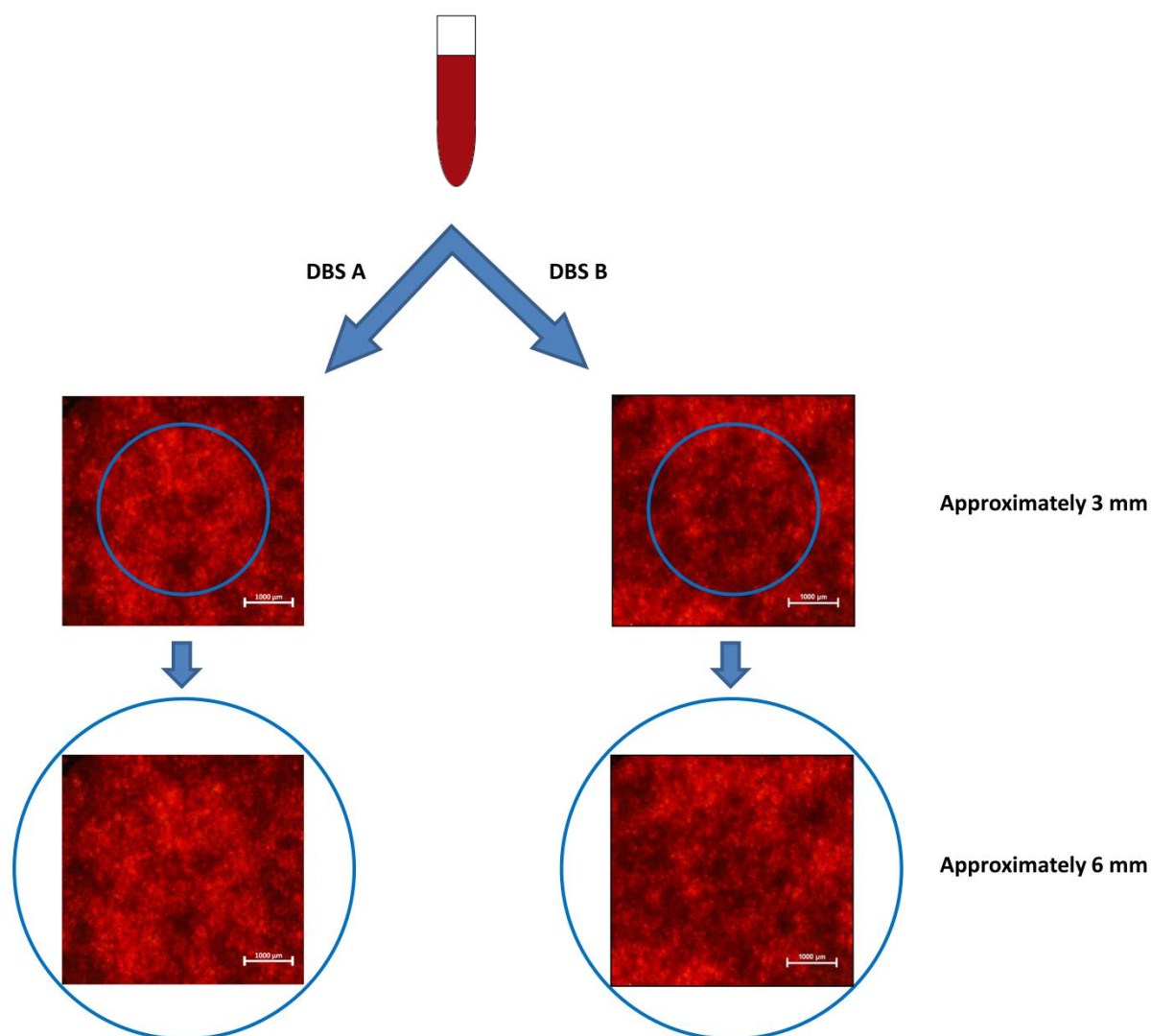
	True Hct	Predicted Hct
Day 1 QC1	0.20	0.223
Day 1 QC2	0.20	0.175
Day 2 QC1	0.21	0.205
Day 2 QC2	0.20	0.208
Day 3 QC1	0.20	0.195
Day 3 QC2	0.20	0.214
Average true Hct	0.202	
SD	0.41	
% bias	0.896%	
% RSD (intra-day)	N.A.	
%RSD (inter-day)	N.A.	

Table S-2B: Normalized true and predicted Hct values.

	True Hct	Predicted Hct
Day 1 QC1	0.202	0.224
Day 1 QC2	0.202	0.177
Day 2 QC1	0.202	0.197
Day 2 QC2	0.202	0.210
Day 3 QC1	0.202	0.196
Day 3 QC2	0.202	0.216
Average true Hct	0.202	
SD	0.00	
% bias	0.896%	
% RSD (intra-day)	10.7%	
% RSD (inter-day)	10.7%	

Supplementary Figure S-3

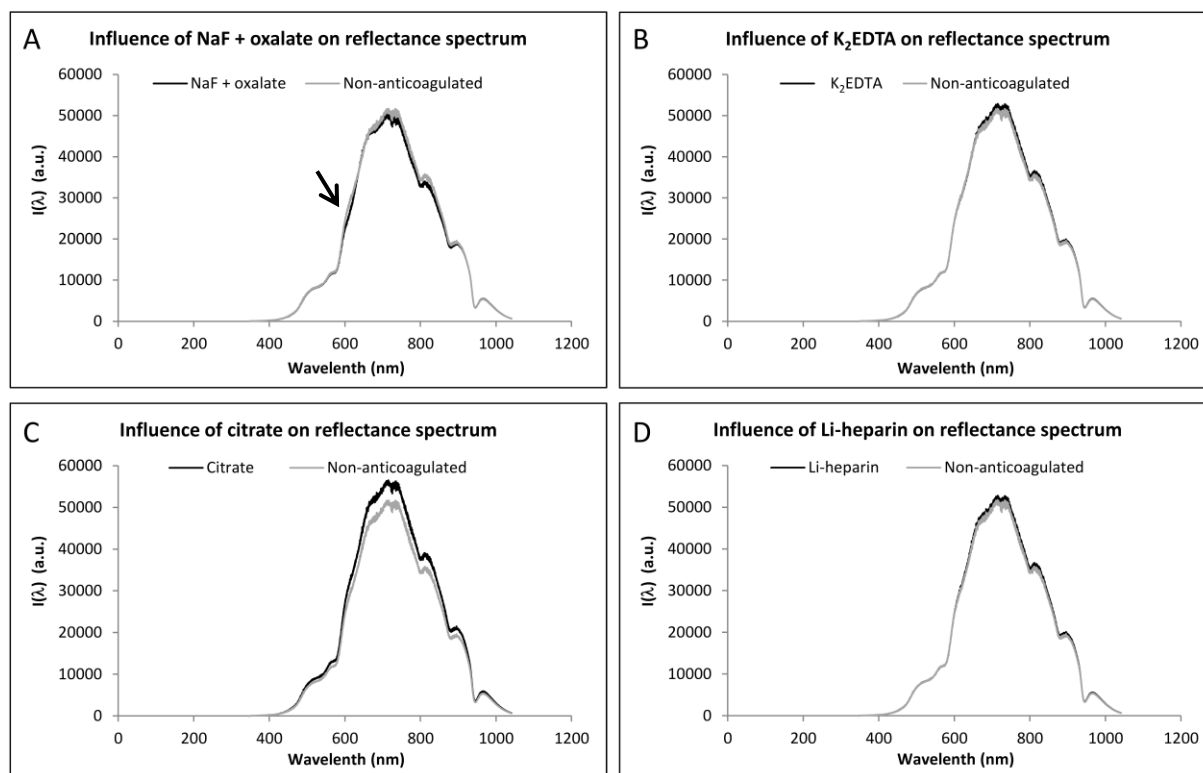
Supporting data regarding the influence of the illuminated spot diameter on method reproducibility. Depicted are images of two DBSs prepared from the same blood source, recorded during light microscopy. A certain degree of inhomogeneity can be observed in the DBSs. Whilst certain areas are darker, others are much lighter, indicating that light can penetrate more easily through the latter areas. These inhomogeneities may impact method reproducibility (at least in the case of a non-contact optical method), especially when the sampled area is relatively small. This can be clearly seen in the images below, as the smaller circles, which represent an illuminated spot with a diameter of 3 mm, clearly encompass almost only lighter areas in DBS A, and only darker areas in DBS B. By increasing the diameter of the sampled area to 6 mm (the larger circles), these inhomogeneities are leveled out (i.e. both 6-mm circles encompass both darker and lighter areas), and method reproducibility improves.



Supplementary Figure S-4A

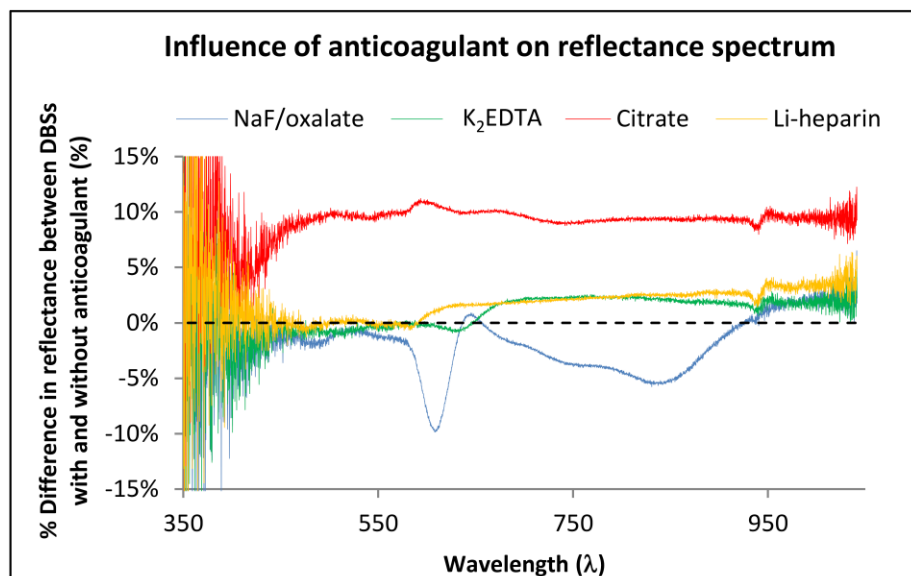
Supporting data regarding the influence of different anticoagulants on the reflectance spectra of DBSs. In each graph the average reflectance spectrum of DBSs without anticoagulant ($n = 6$) is depicted in grey and the average reflectance spectrum of DBSs with anticoagulant ($n = 6$) in black. The anticoagulants that were evaluated are NaF/oxalate (**A**), K_2 EDTA (**B**), citrate (**C**) and Li-heparin (**D**).

The arrow in panel A shows the slightly deviating shape of the reflectance spectrum of NaF/oxalate-anticoagulated blood.



Supplementary Figure S-4B

Supporting data regarding the influence of different anticoagulants on the reflectance spectra of DBSs. Depicted are the percent differences in average reflectance between DBSs with ($n = 6$) and without ($n = 6$) anticoagulant in function of wavelength. The anticoagulants that were evaluated are NaF/oxalate, K_2EDTA , citrate and Li-heparin. While only minor differences can be observed for Li-heparin and K_2EDTA , these differences are more pronounced for citrate and NaF/oxalate.



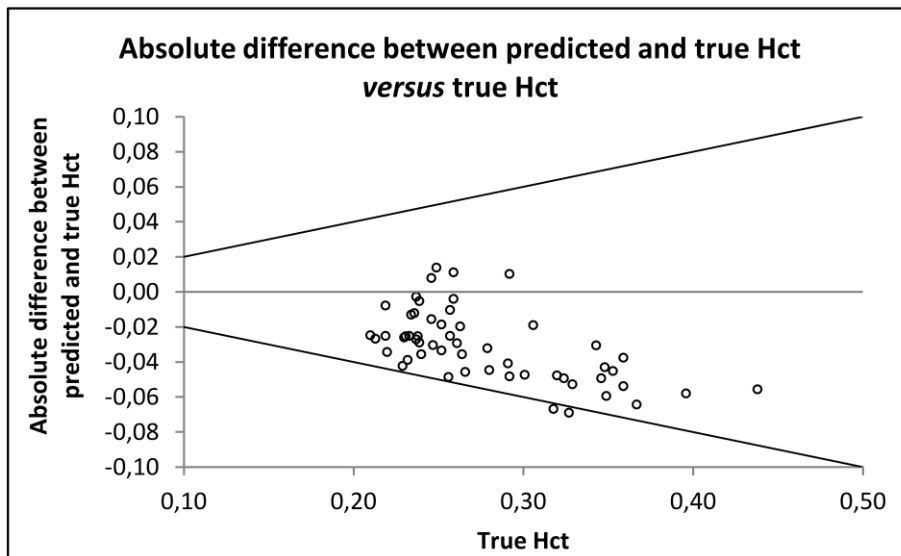
Supplementary Table S-3**Table S-3. Overview of the data for accuracy and precision (n = 6) for donor 2.**

	Accuracy (% bias)	Intraday precision (% RSD)	Interday precision (% RSD)
A) LLOQ	0.386 %	1.73 %	3.80 %
ULOQ	-1.92 %	2.66 %	3.28 %
B) QC LOW	-1.29 %	4.66 %	4.66 %
QC MID	-1.03 %	6.29 %	6.75 %
QC HIGH	-2.25 %	5.19 %	5.19 %
C) QC LOW (donor 1)	1.36 %	6.14 %	7.81 %
QC MID (donor 1)	-4.55 %	4.09 %	4.78 %
QC HIGH (donor 1)	-2.50 %	3.00 %	3.00 %
QC LOW (donor 3)	3.60 %	3.43 %	3.43 %
QC MID (donor 3)	3.24 %	2.16 %	3.17 %
QC HIGH (donor 3)	-0.796 %	3.18 %	3.18 %
QC LOW (donor 4)	2.34 %	5.68 %	5.68 %
QC MID (donor 4)	-1.14 %	9.21 %	9.21 %
QC HIGH (donor 4)	-4.87 %	4.42 %	5.62 %
QC LOW (donor 5)	4.49 %	5.99 %	5.99 %
QC MID (donor 5)	-4.04 %	6.25 %	6.25 %
QC HIGH (donor 5)	-1.76 %	6.64 %	6.64 %
QC LOW (donor 6)	5.25 %	9.17 %	9.17 %
QC MID (donor 6)	2.19 %	11.2 %	11.2 %
QC HIGH (donor 6)	0.778 %	6.22 %	7.62 %

Section A and B respectively give the data obtained for the LOQs (LLOQ and ULOQ) and QCs, prepared from blood of the same donor as the one in which the calibration curves were prepared. Section C gives the data for QCs prepared from blood of five other donors than the one in which the calibration curves were prepared.

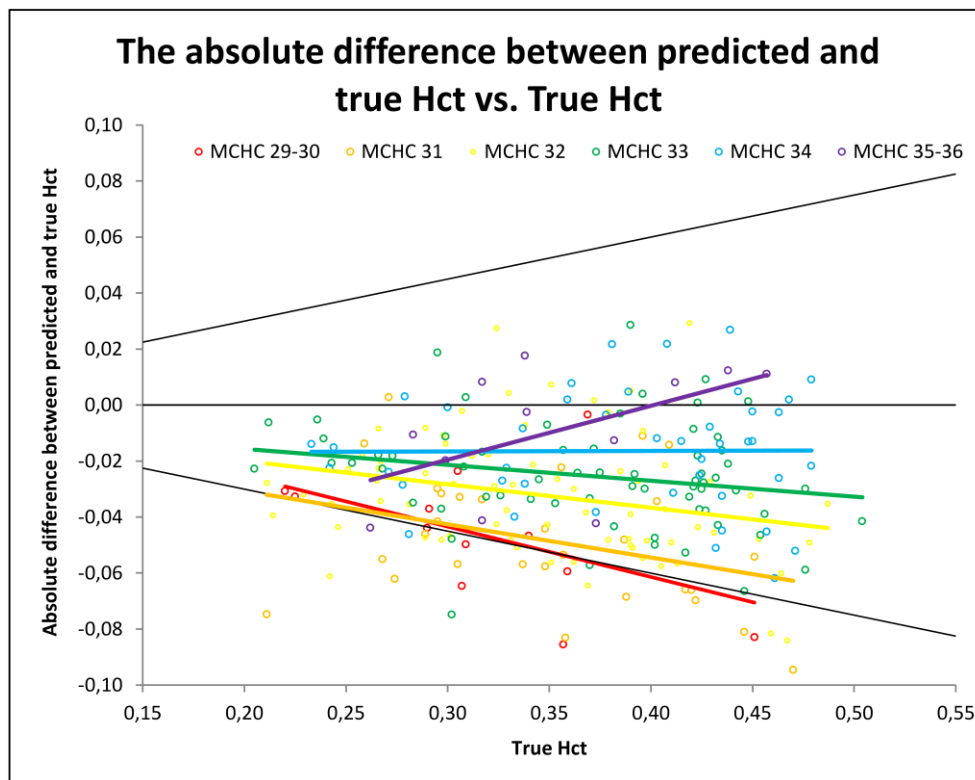
Supplementary Figure S-5

Supporting data regarding the application of the non-contact hematocrit prediction method on Li-heparin anticoagulated DBSs (n = 55). The absolute differences between the predicted and the true patient Hct were plotted against the true patient Hct. The latter Hct values were determined on K₂EDTA-anticoagulated whole blood.



Supplementary Figure S-6

Supporting data regarding the influence of the MCHC value on the predicted Hct. Depicted are the differences in predicted and true hematocrit versus the true hematocrit of the patient samples. The patient samples were divided into different groups based on their MCHC values and each group was assigned a different color. For each group, a trend line in the corresponding color was also incorporated in the figure to facilitate data interpretation. The samples with an MCHC value of 29 or 30 and 35 or 36, respectively, were combined into one group, because of the limited number of samples in these MCHC classes. Also included in the figure are the 15% acceptance criteria, which are depicted by the black lines. Based on the distribution of the patient samples, it can be concluded that the lower the patients' MCHC values were, the more pronounced the underestimation of their Hct values was on average.



Supplementary Figure S-7

The influence of the hemolytic index (panel A & B), lipemic index (panel C & D), and icteric index (panel E & F) on the predicted Hct. In panels A, C en E the percent difference between the predicted and true Hct of the patient samples *versus* the hemolytic, lipemic or icteric index were plotted. In panels B, D and F the absolute differences between the predicted and true Hct of the patient samples were plotted versus the different indexes.

